Fixed-bed adsorption performance and empirical modeling of cadmium removal using adsorbent prepared from the cyanobacterium *Aphanothece sp* cultivar

Awalina Satya [a,b], Ardiyan Harimawan [a], Gadis Sri Haryani [b], M.A.H. Johir [c,*], Luong N. Nguyen [c], Long D. Nghiem [c], Saravanamuthu Vigneswaran [c], Huu Hao Ngo [c], Tjandra Setiadi [a,d,**]

[a] *Department of Chemical Engineering, Faculty of Industrial Technology, Institut Teknologi Bandung, Jl. Ganesa No 10, Bandung 40132, Indonesia*
[b] *Research Center for Limnology, The Indonesian Institute of Sciences- LIPI (P2L-LIPI)- Cibinong Science Center, Jl. Raya Bogor-Jakarta km 46, Bogor 16911, Indonesia*
[c] *Faculty of Engineering and Information Technology, University of Technology Sydney, PO Box 123, Broadway, NSW 2007, Australia*
[d] *Center for Environmental Studies, Institut Teknologi Bandung (PSLH-ITB), Jl. Sangkuriang 42 A, Bandung 40135, Indonesia*

* Correspondence to: School of Civil and Environmental Engineering, University of Technology Sydney, Broadway, NSW 2007, Australia.

** Corresponding author at: Department of Chemical Engineering, Faculty of Industrial Technology, Institut Teknologi Bandung, Jl. Ganesa No 10, Bandung 40132, Indonesia.

E-mail addresses: mohammed.johir@uts.edu.au (M.A.H. Johir), tjandra@che.itb.ac.id (T. Setiadi).

Keywords:
Adsorption
Aphanothece sp
Fixed-bed column
Empirical models
Breakthrough curve

A B S T R A C T

Water contamination by cadmium (Cd), which is a toxic heavy metal widely used in many industrial processes, is a pervasive environmental problem. This study investigated the removal of Cd by dry cyanobacterium *Aphanothece sp* cultivar in adsorption columns The effect of inlet Cd concentrations (1.00 – 4.85mg/L), flow rates (0.30-0.60 L/h) and bed height (4.6 -7.2 cm) on the breakthrough characteristics of the adsorption column was investigated. The maximum adsorption capacity and efficiency were found to be 8.20 mg/g and 89.07 %, respectively with a flow rate of 0.60 L/h and 4.85 mg/L inlet concentration of Cd. The fixed bed adsorption data were fitted to three well known fixed bed empirical models namely Thomas, Adam–Bohart and Yoon–Nelson. The experimental results well fitted with the models mentioned above with R^2 of greater than 0.98 at different conditions. The regeneration efficiency of benthic cyanobacterium *Aphanothece sp* cultivar based adsorbent was studied using 0.1 M HCl. Repetitive adsorption–regeneration experiment show that, at the end of the fifth cycle, the desorption efficiency decreased by 21%. Thus, further research is necessary to improve the reusability of dried biomass of cyanobacterium *Aphanothece sp* adsorbent.

1. Introduction

The cadmium ion (Cd^{2+}) poses a high level of toxicity, therefore hazardous not only to human health but also to the ecological systems and mainly aquatic environments. In the industry, Cd is widely used to produce batteries, metal plating, plastic plasticizers, and color pigments. These activities generate large amounts of Cd-laden wastewaters. Improper treated wastewaters before discharging into open waters, being harmful to the natural environment. Conventional methods

such as ion exchange, flocculation, coagulation, chemical precipitation, and membrane filtration for removing Cd showed varying degree of removal efficiency and are not always cost-effective (Abbar et al., 2019; Ebisike et al., 2019; Talukdar et al., 2020). Adsorption or biosorption using adsorbents made from different biomass could be an alternative and efficient technology for removing Cd from contaminated water (Ahmad and Haydar, 2016; Callery and Healy, 2017; Talukdar et al., 2020)

The use of biosorbent for removing heavy metals is more cost-effective because of its abundant volume, low cost and high biosorption capacity compared to other typical adsorbents (Escapa et al., 2016). Microalgae and cyanobacteria can be grown easily from sunlight, carbon dioxide, and a minute amount of nutrients (Vu et al., 2020a,b). In some cases, they are even considered to be a nuisance in the environment, where algal biomass must be collected and disposed of. Their cell membrane is rich in polysaccharides and sugar functional groups, which can bind different heavy metals. Microalgae biomass is frequently chosen to produce adsorbent or biosorbent since no need to supply any nutrients to grow and has no toxicity risk. Research showed that microalgae dried biomass has high Cd sorption capacity. For example, cyanobacterium of *Oscillatoria sp* based adsorbent or biosorbent showed Cd adsorption capacity of 30.1 mg/g (Katırcıoğlu et al., 2008). On the other hand, green microalgae *Spirogyra insignis* and *Chlorella sorokiniaia* based adsorbents or biosorbents had maximum Cd adsorption capacity of 22.9 and 33.5 mg/g, respectively (Katırcıoğlu et al., 2008; Kumar et al., 2015). Moreover, the adsorbent prepared from dried biomass of *Aphanothece sp.* (cultivated in a photobioreactor system fed with 15% CO_2) showed maximum biosorption capacity of Cd of 60.24 mg/g when implemented on batch biosorption system (Satya et al., 2020, 2017). However, data on Cd sorption from aqueous solution using adsorbents produced from cyanobacteria are still very limited. However, the cyanobacteria are more easily grown and have better adsorption capacity of heavy metals than other microalgae phyla.

Among of different adsorption process, the fixed bed column adsorption process is preferable (than batch process) as it can be conducted continuously for successive adsorption–desorption cycles for a longer time. Also, the continuous column adsorption system gave more accurate sorbent capacity of the adsorbent and the data generated from column adsorption study help to design pilot-scale column adsorption for industrial application (Abdolali et al., 2017; González-López et al., 2020).

In this study, adsorbent prepared from *Aphanothece sp* biomass was tested using a fixed-bed column. Emphasis was given on finding the adsorption maximum capacity and efficiency, which is very vital when running continuous column for practical application. Three empirical models (Thomas, Adam–Bohart, and Yoon–Nelson) were used to describe the experimental breakthrough curves and to obtain design parameters (kinetics rate and maximum biosorption capacity). The adsorption–desorption study was also conducted for five cycles to study the feasibility of regenerating the spent adsorbent.

2. Material and methods

2.1. Biomass and chemicals

The isolate living biomass of *Aphanothece sp* taken from Lake Situ Rawa Kalong (Depok City-West Java, Indonesia). Naturally, this cyanobacterium was capable of accumulating cadmium ions in its biomass up to 4,150 times higher from its surrounding waters (Satya et al., 2018).

After collecting the cyanobacterium *Aphanothece sp,* it was isolated and cultivated in BG-11 medium in a photobioreactor system (under the illumination of 1000 lux, at a temperature of 28–30 °C) (Andersen, 2005). Afterwards, cultivation was done using the irradiation of ∼5700–6000 lux (∼114 - 120 μmol. photon/m^2/s) while incubated at a temperature ranging between 26.1 – 29.1 °C for 14 days and intermittently fed with airstream enriched with 15% of CO_2 gas for 6 h each day. The harvested biomass dewatered by centrifugation at 6000 rpm for 15 min, followed by an oven-dry at 60 °C for 7 days to achieve a constant weight of dry biomass. The dried biomass then grinds and sieved. The produce adsorbent had an average particle size of 40 μm (particle diameter was in the ranges of 5.5 to 82.6 μm). The surface area, average pore diameter and pore volume were 1.735 (m^2/g), 111.29 (Å) and 4.74 × 10^{-3} cm^3/g, respectively.

2.2. Fixed bed column experiment

The schematic of the fixed-bed adsorption column experiment is presented in Fig. 1. Fixed bed column adsorption experiments were conducted using a glass column having an internal diameter and height of 2 and 20 cm, respectively. To overcome the walls influencing problem, the ratio of the column to particle diameter was kept higher than 10 (Beni and Esmaeili, 2020; Worch, 2012). White plastic wool (3 cm height) was placed at the bottom and top of the fixed bed column to pack the adsorbent. A clear plastic screen (pore size 0.3 mm) was placed between the adsorbent bed and plastic wool to prevent adsorbent loss and bed movement. An upward flow mode of operation was employed at a constant flow rate using a pump, and sampling was done at the column outlet at specified intervals.

A certain amount of cadmium salt ($CdCl_2$.2.5 H_2O) was dissolved in demineralized water for preparing the required feed solution. The pH of the feed water was adjusted to 8 using KH_2PO_4 buffer solution at ambient room temperature of 28–30 °C. This pH was chosen based on the previous study, and this pH was optimum (Satya et al., 2020). Sets of sorption column experiments were conducted to evaluate the effects of (i) different bed heights (4.6, 5.4 and 7.2 cm); (ii) volumetric

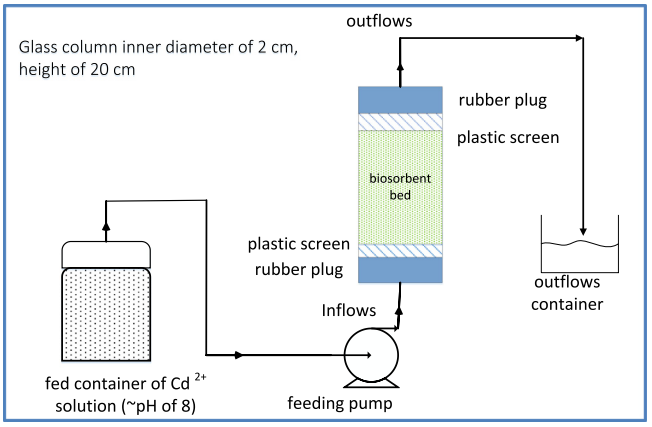

Fig. 1. The scheme of fixed-bed adsorption column experiment.

flows of 0.30, 0.42 and 0.60 L/h; and (iii) four initial Cd concentrations (1.05, 1.86, 3,59 and 4.85 mg/L). The desired bed height was achieved by packing 1.35, 1.53 and 1.8 g of adsorbent. Sampling was done at certain time intervals (5–590 min), and residual Cd concentrations were measured using Flame Atomic Absorption Spectrophotometer (FAA) (AA-7000 series, Shimadzu, Japan) shows on manual instruction of the FAA instrument. $CdCl_2.2.5\ H_2O$ (M&B Chemical), all chemicals used were analytical grade (Merck, Darmstadt, Germany).

2.3. Bed regeneration experiments

After saturation of the absorbent, regeneration must be conducted to use the adsorbent for several cycles which will be more economical (Ahmad and Haydar, 2016; Bulgariu and Bulgariu, 2016). In this study, 0.1 M HCl desorbing solution was used to the regenerated adsorbent bed, and the regenerated adsorbent was reused for the next cycles (after regeneration the adsorbent was rinsed with demineralized water, pH of ~7). Adsorption–desorption experiments were conducted for five cycles. After regeneration, the adsorption and desorption capacities and removal efficiencies in every cycle were also assessed.

2.4. Experimental data analyzing

The breakthrough curve was produced by plotting the normalized concentrations (C_t/C_o) versus time to investigate the adsorption behavior of Cd on to adsorbent in a fixed-bed column. A steep breakthrough curve with a short mass transfer zone (MTZ) is favored since it suggests a longer service time and more effective use of the adsorbent (Mazur et al., 2016). In this study breakthrough time (t_b) was calculated when the normalized concentration of Cd reached to 0.05. This value is chosen since the average Cd concentration in electroplating wastewater is 0.96 mg/L (Xu et al., 2013) and in Indonesia, the regulatory standard for Cd contained in industrial wastewater is 0.05 mg/L (KLH, 2014). The saturation time (t_s) was calculated when the normalized concentration of Cd becomes almost 1.

The total volume of treated effluent (V_{eff}), Cd mass sorbed/attached in an adsorbent bed (q_{total}), the total mass of Cd passing through the column (m_{total}), adsorption capacity ($q_{max,col}$), removal efficiency (% EB) and the empty bed contact time (EBCT) were calculated based on Eqs. (1) to (6)

$$V_{eff} = Q \times t_{total} \tag{1}$$

$$q_{total} = \frac{Q}{1000}\int_{t_0}^{t_{total}} C_{ads}dt = \frac{Q}{1000}\int_{t_0}^{t_{total}} \left(C_{inf} - C_t\right) dt \tag{2}$$

$$m_{total} = C_{inf}Q \tag{3}$$

$$q_{max,col} = \frac{q_{total}}{M} \tag{4}$$

$$\%\ EB = \frac{q_{total}}{m_{total}} \times 100 \tag{5}$$

$$EBCT = \frac{bed\ volume(mL)}{Q(\frac{mL}{minute})} \tag{6}$$

where Q, C_{inf}, and q_{total} are volumetric flow rate (L/h); Cd concentration in the influent (mg/L); and total mass of Cd sorbed in the adsorbent (mg).

2.5. Empirical modeling

Modeling on a fixed-bed column is used to calculate design parameters and predict the breakthrough behavior adsorption column (which called as dynamic properties) for scaling-up purposes and performance comparison. The process of sorption in the fixed bed is quite complex since it involves several factors such as the axial dispersion, sorption kinetics, mass transfer, and intraparticle diffusion resistance hence requires a series of non-linear partial differential equations (Burkert et al., 2011). Therefore, simplified semi-empirical models such as Thomas Eq. (7), Adam–Bohart Eq. (8) and Yoon–Nelson Eq. (9) have frequently been employed for describing the experimental breakthrough data (Callery and Healy, 2017; Chatterjee et al., 2018).

Calibration on Thomas, Adam–Bohart and Yoon–Nelson models used real-time data set through the non-linear square method. A non-linear squares method was employed using Solver-add MS-Excel TM to obtain the best fit and all model parameters (K_{Th}, $q_{max,col}$, K_{AB}, N_0, k_{YN} and τ) based on the magnitude of the coefficient of determination (R^2). Eq. (10).

$$\frac{C}{C_i} = \frac{1}{1 + exp\left[\left(\frac{K_{Th}}{Q}\right)\left(q_{max,col}M - C_i tQ\right)\right]} \tag{7}$$

Where C and C_i are the effluent and influent cadmium concentration (mg/L), K_{Th} is Thomas rate constant (L/mg.min).

$$\frac{C}{C_i} = \frac{1}{1 + exp\left[\frac{(K_{AB}N_0 Z)}{\upsilon} - K_{AB}C_i t\right]} \tag{8}$$

C and C_i are the Cd concentrations at the fixed bed outflow and inflow, K_{AB}, N_0, Z, υ is the rate constant of Adam–Bohart; sorption capacity of sorbent per unit volume of the bed; total bed depth; and the superficial velocity. The parameters K_{AB} and N_0 are fitting parameters.

$$\frac{C}{C_i} = \frac{exp\,(K_{YN}t - K_{YN}\tau)}{1 + exp\,(K_{YN}t - K_{YN}\tau)} \tag{9}$$

Where K_{YN} *and* τ are the Yoon–Nelson model rate constant (/minute) and the time that $\frac{C}{C_i}$ is equal to a value of 0.50. The unknown parameters K_{YN} and τ are obtained using direct fitting of the model to the experimental data via the non-linear least squares' method.

The value coefficient of the determinant (R^2) (calculated as Eq. (10)) ranges between 0 and less than 1, denotes the strength of the association between experimental data and predicted data (represents the percentage of closeness).

$$R^2 = 1 - \frac{\sum_{n=1}^{n}\left(\left(\frac{C_t}{C_{inf}}\right)_{eksp,n} - \left(\frac{C_t}{C_{inf}}\right)_{model,n}\right)^2}{\sum_{n=1}^{n}\left(\left(\frac{C_t}{C_{inf}}\right)_{eksp,n} - \overline{\left(\frac{C_t}{C_{inf}}\right)_{model,n}}\right)^2} \tag{10}$$

The non-linear error functions used in this study are the Residual Root Mean Square Error (RMSE; Eq. (11)) and the Chi-Square test (X^2; Eq. (12))

$$RMSE = \sqrt{\frac{1}{n-1}\sum_{n=1}^{n}\left(\left(\frac{C_t}{C_{inf}}\right)_{eksp,n} - \left(\frac{C_t}{C_{inf}}\right)_{model,n}\right)^2} \tag{11}$$

$$\chi^2 = \sum_{n=1}^{n}\frac{\left(\left(\frac{C_t}{C_{inf}}\right)_{eksp,n} - \left(\frac{C_t}{C_{inf}}\right)_{model,n}\right)^2}{\left(\frac{C_t}{C_{inf}}\right)_{model,n}} \tag{12}$$

The smaller value of both RMSE and χ^2 suggest the better model fitting and the similarity between experimental data and model.

3. Results and discussion

3.1. Effect of bed height on Cd adsorption

Adsorption of Cd ions in the fixed bed column is mostly dependent on the quantity of adsorbent used in the column. The adsorption breakthrough curves obtained at different bed height is presented in Fig. 2. As expected, increasing bed height prolonged breakthrough and exhaustion time, since more binding sites became available for biosorption consequently followed by more extended mass transfer zone. The number of bed volume treated at 50% saturation with a different bed height of 4.6, 5.4, and 7.2 cm were 61, 73 and 80, respectively. However, the overall maximum adsorption capacity tends to decrease as bed height increase due to an increase in the mass of adsorbent (Table 1). It means that as the bed height

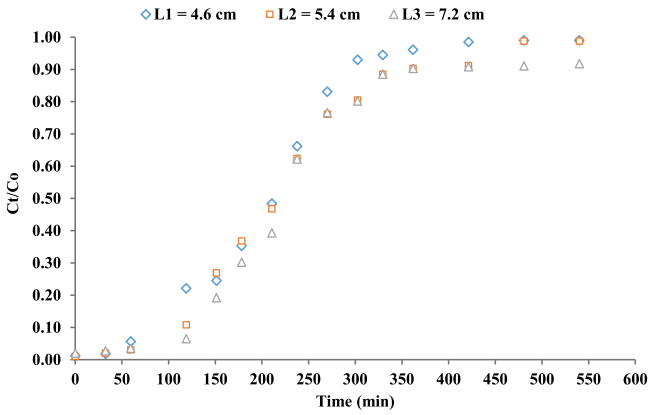

Fig. 2. Breakthrough curves for Cd adsorption at different bed heights (flow rate = 0.30 L/h, initial cadmium concentration = 1.05–1.08 mg/L, pH = 8).

Table 1
Process parameter and experimental data of the fixed bed adsorption system operated at different conditions.

No.	Parameter	Symbol	Unit	Varied operational condition									
				A. Bed height (cm)[a]			B. Volumetric flows (L/h)[b]			C. Initial concentration of Cd^{2+}(mg/L)[c]			
				L1 = 4.6	L3 = 5.4	L4 = 7.2	Q1 = 0.30	Q2 = 0.42	Q3 = 0.60	C1 = 1.05	C2 = 1.86	C3 = 3.59	C4 = 4.85
1	The total volume of treated effluent	V_{eff}	L	2.70	2.70	2.70	2.70	3.80	5.40	2.70	2.70	2.70	2.70
2	Total passed through of Cd	$m_{totalCd}$	mg	2.83	2.83	2.83	4.72	5.65	9.52	2.83	5.02	9.69	13.09
3	Total adsorbed Cd	$q_{totalCd}$	mg	1.73	2.10	3.92	2.10	3.92	8.48	1.51	3.14	6.90	9.84
4	The maximum adsorption capacity	$q_{max,column}$	mg/g	1.53	1.75	3.27	1.75	3.27	7.07	1.26	2.62	5.75	8.20
5	Adsorption efficiency of the column	% R_{column}	%	61.07	64.37	69.45	44.37	69.45	89.07	53.24	62.46	71.18	75.18
6	Dried weight of adsorbent	M	gram	1.21	1.36	1.81	1.20	1.20	1.20	1.20	1.20	1.20	1.20
7	Breakthrough time	t_b	second	3564	5236	6545	6614	1889	619	9072	5461	2868	1068
8	Equilibrium time	t_e	second	22909	24218	25909	23492	19988	10692	22175	17892	16200	8847
9	Empty Bed Contact Time	EBCT	second	173	201	271	188	134	94	188	188	188	188
10	Mass Transfer Zone	MTZ	cm	3.86	4.21	4.81	3.45	4.75	4.84	4.14	4.29	4.35	4.66

[a]Initial concentration of Cd = 1.05–1.08 mg/L, flow = 0.30 L/h.
[b]Initial Cd = 1.05–1.08 mg/L, bed height = 5 cm.
[c]Flow = 0.30 L/h, bed height = 5 cm.

increased (1.5-fold), the mass transfer resistance also increased, which may reduce adsorption capacity. It also suggested that mass transfer resistance could not be overcome at a flow rate of 0.30 m^3/h (superficial flow of 2.83 cm/min). A similar trend also reported by Muhamad et al. (2010). In their study, they used a wheat straw (*Triticum sativum*) in a fixed bed column for treating Cd^{2+} in synthetic wastewater.

3.2. Effect of flow rate on Cd adsorption

On an industrial scale, a continuous wastewater treatment using the adsorption system, the flow rate is a major factor which must be evaluated. A steeper breakthrough curve, faster bed saturation, and shorten EBCT were observed with an increase in the flow rate (Fig. 3 and Table 1). At low flow rate (0.30 L/h) the number of bed volume treated (at 50% saturation) was 74 which is almost 2 times higher than that of the high flow rate of 0.6 L/h. However, overall the maximum sorption of Cd increased with an increase in flowrate. At a higher flow rate, the mass transfer rate increases, thus the amount of Cd adsorbed on the unit mass of adsorbent bed (mass transfer zone) also increased (Worch, 2012).

The breakthrough time decreased significantly by up to ten times was observed when the flow rate was doubled. This indicates that adsorption includes two stages which dominated the overall removal of Cd. In the first stage, Cd moved from the bulk solution to the adsorbent surface followed by adsorption of Cd on the adsorbent's surface by overcoming the film resistance surrounding the adsorbent particle. Thus, external mass transfer controlled adsorption in a fixed bed column. This finding aligns with the work done by Vijayaraghavan and Yun (2008). They found that if the external mass transfer controls the adsorption process, it must be managed with a higher flow rate to reduce the external and film mass transfer resistance.

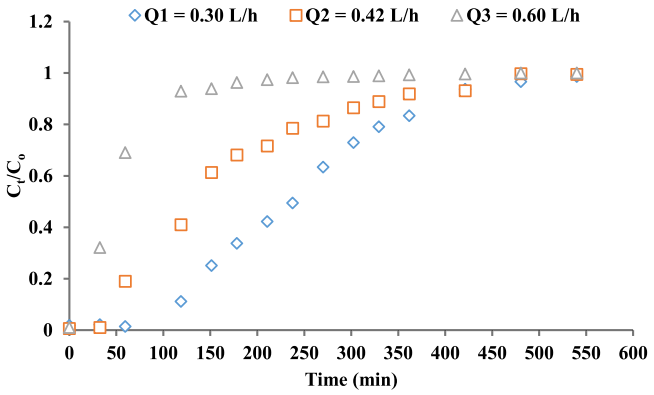

Fig. 3. Breakthrough curves for cadmium adsorption different volumetric flow (bed height = 5 cm, initial cadmium concentration = 1.49–1.76 mg/L, pH = 8). Colored arrows depict the breakthrough steepness.

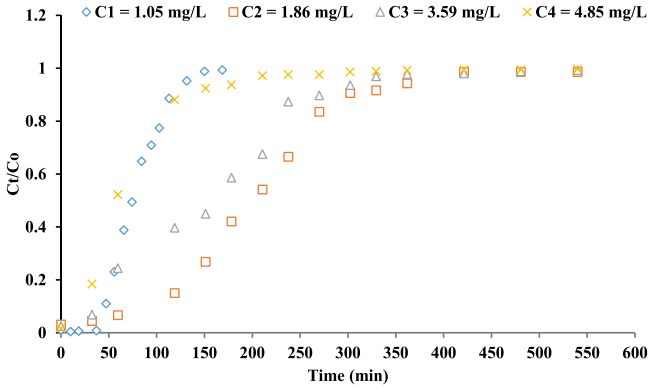

Fig. 4. Breakthrough curves for cadmium biosorption at different inlet Cd concentration (bed height = 5 cm, flow rate= 0.30 L/h, pH = 8).

In the present study, the adsorption capacity (7.07 mg/g) was almost 14 times lower than reported data (101.61 mg/g) Jafari and Jamali (2016) who used adsorbent produced from *Sargassum angustifolium* dried biomass. This could be due to: (i) being caused by the different operational conditions such as the influent concentration of Cd of 65 mg/L (60-times more concentrated than present study); and (ii) operating flow rate of 1.80 m^3/h which is six times higher than the flow rate used in this study. The differences were also probably caused by the characteristics (quantitatively and qualitatively) of the adsorbent as well as the bulk solution's sorbate properties (Amirnia et al., 2016; Jafari and Jamali, 2016).

3.3. Effect of Cd concentration on adsorption

The influent concentration of Cd affected the fixed bed's performance, which was evident from the breakthrough curves presented in Fig. 4. At lower influent Cd concentration of 1.05 mg/L the number of bed volume treated was 74 (at 50% saturation) whereas it was only 18 with an influent Cd concentration of 4.85 mg/L. However, the adsorption capacity increased with increase with the increase in influent Cd concentration (Table 1). A similar phenomenon was reported on the adsorption of copper using adsorbent prepared from *Posidonia oceanica* biomass (Izquierdo et al., 2010). The lower concentration gradient leads to slower transport of Cd from the bulk solution to the adsorbent surface due to lower mass transfer coefficient (Amirnia et al., 2016). Moreover, at higher initial Cd concentration, the binding sites of the adsorbent get exhausted much faster as reported by a various researcher (Abbar et al., 2019; Ebisike et al., 2019; Jafari and Jamali, 2016). Therefore, it can be concluded that the initial Cd concentration strongly influenced the fixed bed adsorption column's performance.

3.4. Empirical model fitting and parameter

The experimental data were fitted with widely use three empirical models of Thomas, Adam–Bohart and Yoon–Nelson as described below.

Table 2
Different empirical model parameters at varying adsorbent bed depths.

Thomas model	Q (L/h)	C_{inf} (mg/L)	L_{bed} (cm)	K_{TH} (mL/mg min)	$q_{max,model}$ (mg/g)	$q_{max,exp}$ (mg/g)	R^2	RMSE	χ^2
	0.30	1.05	4.60	19.74	0.89	1.57	0.994	0.004	0.052
	0.30	1.09	5.40	9.73	1.55	1.22	0.995	0.012	0.052
	0.30	1.08	7.20	20.11	0.73	0.78	0.992	0.011	0.070
Adam–Bohart model	Q (L/h)	C_{inf} (mg/L)	L_{bed} (cm)	K_{AB} (L/mg min)	$N_{0,model}$ (mg/L)		R^2	RMSE	χ^2
	0.30	1.05	4.60	0.020	133.15	0.994	0.004	0.052	
	0.30	1.09	5.40	0.010	207.85	0.995	0.010	0.052	
	0.30	1.08	7.20	0.012	198.81	0.992	0.011	0.070	
Yoon–Nelson model	Q (L/h)	C_{inf} (mg/L)	L_{bed} (cm)	K_{YN} (1/min)	τ_{model} (min)	τ_{exp} (min)	R^2	RMSE	χ^2
	0.30	1.05	4.60	0.021	204.18	207	0.994	0.004	0.052
	0.30	1.09	5.40	0.018	214.38	216	0.995	0.010	0.052
	0.30	1.08	7.20	0.022	205.05	201	0.992	0.011	0.070

3.4.1. Empirical models fitting at different bed heights

Breakthrough curves of the experimental data resulting from different bed heights variation were fitted with three empirical models (Electronic Annex). The breakthrough curves of the models and experimental data were in good agreement based on R^2, RMSE and X^2 values (Table 2). This means that Thomas, Adam–Bohart and Yoon–Nelson models can be used to describe the dynamic behavior of the column. Thomas model was developed from mass conservation in a flow system. It assumes that the biosorption process follows the second-order reaction kinetic, while adsorption equilibrium complied with the Langmuir model without axial dispersion. This empirical model can be used to predict the breakthrough curve and the maximum uptake of the sorbate by biosorbent. While Adam–Bohart model is based on the assumption that sorption proceeds continuously wherein equilibrium is not achieved instantaneously. The sorption kinetic is proportional to the sorption capacity of sorbent. The Yoon–Nelson model is the most specific (least column parameters and data) compared to Thomas and Adam–Bohart models. It was developed based on adsorption theory and the breakthrough of adsorbate probability. Furthermore, it applies to a monometallic system (Jafari and Jamali, 2016). Therefore, this study chooses these three empirical models to comprehend the dynamic behavior of the column.

Thomas kinetic constants increased with an improvement in bed height, but adsorption capacity decreased, probably due to mass transfer resistance being greater as bed height increased. The q_{max} of the Thomas model showed only a minor difference to the experimental data. The value of N_0 decreased with the increase in the adsorbent bed height due to more active sites being available for Cd biosorption. However, the K_{A-B} decreased as bed height increased, which suggested that more mass transfer resistance occurred. The values of K_{Y-N} were and predicted 50% breakthrough time did not vary significantly with the variation in bed height.

3.4.2. Empirical models fitting at a different volumetric flow rate

The steepness of breakthrough curves rises with the increase in flow rates (Electronic Annex). The value of K_{Th} increased 4.4 times when the flow rate was increased two-folds (Table 3). Unfortunately, the value of experimental q_{max} did not confirm the value of q_{max} as predicted in the Thomas model. A similar pattern also observed for the Yoon–Nelson model, and a 50% difference was found for a breakthrough time obtained from experiment and model date. The Adam–Bohart model provided a comparable pattern like the previous two models, which can be deduced from the relevant R^2, RMSE and X^2 values. These findings show that three empirical models are not suitable to describe the experimental data at volumetric flows.

3.4.3. Empirical models fitting at different influent Cd concentration

Based on R^2, RMSE, and X^2 values (Table 4), the breakthrough curves were well fitted with three models fitted used in this study. This implies the dynamic behavior of the biosorption process can be explained by the models used in this study and this also aligns with the previous findings where they also used Thomas, Adam–Bohart and Yoon–Nelson (Jafari and Jamali, 2016). The increase in influent Cd concentration resulted in steeper breakthrough curves (Electronic Annex) and the value of K_{Th} decreased when the increase in influent concentration, while q_{max} increasing (Table 4). It indicates that the mass transfer that occurred in the fixed bed system contributed to the sorption kinetics.

The value of K_{A-B} decreased two-fold as the influent Cd concentration increased (Table 4). Unlike this, the N_0 value decreased together with the initial Cd concentration due to more Cd being adsorbed in the adsorbent bed. Higher influent Cd concentration led to a higher driving force for Cd ions passing through the external film, which facilitated the Cd ions having access to active sites on the sorbent's surface (Callery and Healy, 2017). Similar to the Adam–Bohart model, the K_{Y-N} also tended to increase with an increase in the influent Cd concentration (Table 4). The values of predicted 50% breakthrough times from model data were very close with the experimental results.

Table 3
Different empirical model parameters at varying volumetric flow rates.

Thomas model	Q (L/h)	C_{inf} (mg/L)	L_{bed} (cm)	K_{TH} (mL/mg min)	$q_{max,modelNL}$ (mg/g)	$q_{max,exp}$ (mg/g)	R^2	RMSE	χ^2
	0.30	1.75	5	8.64	1.02	1.75	0.995	0.007	0.083
	0.42	1.49	5	9.06	1.52	3.27	0.968	0.023	0.233
	0.60	1.76	5	37.98	0.54	7.07	0.988	0.019	0.064
Adam–Bohart model	Q (L/h)	C_{inf} (mg/L)	L_{bed} (cm)	K_{AB} (L/mg min)	$N_{0,model}$ (mg/L)		R^2	RMSE	χ^2
	0.30	1.32	5.0	0.008	387.59	0.995	0.007	0.083	
	0.42	1.49	5.0	0.009	243.13	0.968	0.023	0.234	
	0.60	1.76	5.0	0.038	80.78	0.988	0.020	0.064	
Yoon–Nelson model	Q (L/h)	C_{inf} (mg/L)	L_{bed} (cm)	K_{YN} (1/mi)	τ_{model} (min)	τ_{exp} (min)	R^2	RMSE	χ^2
	0.30	1.32	5.0	0.015	235.05	240	0.995	0.007	0.083
	0.42	1.49	5.0	0.016	148.01	97	0.968	0.023	0.234
	0.60	1.76	5.0	0.057	45.55	15	0.988	0.020	0.064

Table 4
Different empirical model parameters varying influent Cd concentrations.

Thomas model	Q (L/h)	C_{inf} (mg/L)	L_{bed} (cm)	K_{TH} (mL/mg min)	$q_{max,modelNL}$ (mg/g)	$q_{max,exp}$ (mg/g)	R^2	RMSE	χ^2
	0.30	1.05	5.0	17.83	1.08	1.26	0.993	0.009	0.124
	0.30	1.86	5.0	17.91	1.79	2.62	0.980	0.037	0.106
	0.30	3.59	5.0	4.79	2.29	5.75	0.989	0.002	0.092
	0.30	4.85	5.0	1.26	8.46	8.20	0.990	0.019	0.058
Adam–Bohart model	Q (L/h)	C_{inf} (mg/L)	L_{bed} (cm)	K_{AB} (L/mg min)	$N_{0,model}$ (mg/L)		R^2	RMSE	χ^2
	0.30	1.05	5.0	0.018	143.13	0.993	0.009	0.124	
	0.30	1.86	5.0	0.021	153.00	0.996	0.008	0.100	
	0.30	3.59	5.0	0.005	316.77	0.989	0.002	0.092	
	0.30	4.85	5.0	0.039	36.44	0.990	0.019	0.058	
Yoon–Nelson model	Q (L/h)	C_{inf} (mg/L)	L_{bed} (cm)	K_{YN} (1/min)	τ_{model} (min)	τ_{exp} (min)	R^2	RMSE	χ^2
	0.30	1.05	5.0	0.019	245.65	239	0.993	0.009	0.124
	0.30	1.86	5.0	0.020	199.64	190	0.998	0.006	0.024
	0.30	3.59	5.0	0.017	153.58	152	0.989	0.002	0.092
	0.30	4.85	5.0	0.041	62.54	61	0.990	0.019	0.058

3.5. Regeneration of exhausted adsorbent

The exhausted adsorbent bed should be regenerated for enabling the adsorbent reusability and recovery of adsorbed Cd. The reusability of the adsorbent usually assessed by observing successive study on adsorption–desorption (A–D) for several cycles (Beni and Esmaeili, 2020). In this study, the percentages of A–D values were calculated concerning the original amount of adsorbent. Table 5 shows that the result was quite promising and proved that adsorbent produced from *Aphanothece sp.* dried biomass could be used repeatedly without significant loss of adsorption capacity for Cd. There was only a slight decline in adsorption efficiency (0.53%). The desorption efficiency reduced by around 13.01% after five cycles. Furthermore, the desorption process was practically completed after 2 h. A reduction in desorption efficiency was attributed to deterioration of surface ligands (active binding sites) for Cd by the desorbing solution. The deterioration process was evident in the diminishing capacity which ranged from: firstly, 1.13–1.36 mg/g for adsorption; and secondly, 0.66–0.69 mg/g for desorption. The reduced accessibility on binding sites led to a faster breakthrough. However, both adsorption and desorption capacities were almost the same for five cycles. The Cd adsorption process strongly depended on the previous desorption process. More prolonged contact of adsorbent with 0.1 M HCl desorbing solution during the regeneration process gradually damage or deactivated the adsorbent Afterwards, the recovery of Cd from desorbing eluent can be conducted by applying conventional methods such as electrodeposition, electrolysis, or precipitation (Mazur et al., 2016).

Table 5
Process parameters for five consecutive adsorption–desorption cycles (flow rate = 0.3 L/h and a bed height = 5 cm; desorbing eluent was 0.1 M HCl).

No.	Parameter	Symbol	Cycles				
			A–D1	A–D2	A–D3	A–D4	A–D5
1	The concentration of Cd in influent (mg/L)	C_{inf}	1.05	1.05	1.05	1.36	1.26
2	Total adsorbed Cd (mg)	q_{total}	1.37	1.58	1.54	2.11	1.63
3	Total of passed through Cd (mg)	m_{total}	2.84	3.67	3.29	3.4	3.4
4	Breakthrough time (minute)	t_b	100	100	100	90	90
5	Saturation time (minute)	t_s	410	420	410	420	410
6	Mass Transfer Zone (cm)	MTZ	3.78	4.88	3.05	3.93	3.90
7	The maximum biosorption capacity (mg/g)	$q_{max.}$	1.13	1.31	1.27	1.36	1.34
8	The efficiency of Cd adsorption (%)	EB	48.34	43.13	46.73	47.71	47.81
9	The maximum desorption capacity (mg/g)	$q_{max.des.}$	0.69	0.68	0.68	0.69	0.66
10	The efficiency of desorption (%)	ED	61.78	52.16	53.34	50.74	48.77

4. Conclusions

The fixed bed adsorption finding showed that the adsorbent produced from *Aphanothece sp* dried biomass was capable of removing Cd from aqueous solution. Better Cd removal was achieved with low inlet Cd concentration, high adsorbent bed height and low influent flow rate. The number of bed volume treated with different bed heights was in the ranges between 60 to 80. Furthermore, with a flow rate of 0.30 L/h and at 50% saturation, the number of bed volume treated 2 times higher than that of the high flow rate of 0.6 L/h. This finding can be deducted from the difference between a predicted parameter and experimental parameter which lead to distinction on to each of the relevant R^2, RMSE and X^2 values. These models can be implemented to evaluate the strength and weakness of *Aphanothece sp* dried biomass as a sorbent for removing cadmium ions in aqueous solution using Fixed bed biosorption system. The adsorption capacities in five consecutive adsorption–desorption cycles were almost constant. Furthermore, the desorption capacities and desorption efficiencies were reduced by 4% and 20%, respectively at the end of five cycles. This method can benefit Cd concentrating and sequestering when required in the future.

CRediT authorship contribution statement

Awalina Satya: Conceptualized the project design, Prepared biosorbent and executed work, Performed modeling on the data, Contributed in the final draft of the manuscript, Review and edit process. **Ardiyan Harimawan:** Conceptualized the project design, Performed modeling on the data, Contributed in the final draft of the manuscript, Review and edit process. **Gadis Sri Haryani:** Contributed in the final draft of the manuscript, Review and edit process. **M.A.H. Johir:** Performed modeling on the data, Contributed in the final draft of the manuscript, Review and edit process, Submit the manuscript. **Luong N. Nguyen:** Contributed in the final draft of the manuscript, Review and edit process. **Long D. Nghiem:** Contributed in the final draft of the manuscript, Review and edit process. **Saravanamuthu Vigneswaran:** Contributed in the final draft of the manuscript, Review and edit process. **Huu Hao Ngo:** Contributed in the final draft of the manuscript, Review and edit process. **Tjandra Setiadi:** Conceptualized the project design, Performed modeling on the data, Contributed in the final draft of the manuscript, Review and edit process, Submit the manuscript.

Declaration of competing interest

The authors declare that they have no known competing financial interests or personal relationships that could have appeared to influence the work reported in this paper.

Acknowledgment

The authors are very grateful to the PRN-Malsai Fiscal Year of 2020 (Mikro-Makroalga Strain Asli Indonesia-The Native Strain of Indonesian Micro and Microalgae National Research Priority Project) of The Indonesian Institute of Sciences for providing facilities. Furthermore, the first author acknowledges the financial support provided by the Institute. Collaboration with the University of Technology Sydney is financially supported by the grantsponsor World Class University - 2020 Program of Institut Teknologi Bandung.

Appendix A. Supplementary data

Supplementary material related to this article can be found online at https://doi.org/10.1016/j.eti.2020.101194.

References

Abbar, A.H., Salman, R.H., Abbas, A.S., 2019. Cadmium removal using a spiral-wound woven wire meshes packed bed rotating cylinder electrode. Environ. Technol. Innov. 13, 233–243.

Abdolali, A., Ngo, H.H., Guo, W., Zhou, J.L., Zhang, J., Liang, S., Chang, S.W., Nguyen, D.D., Liu, Y., 2017. Application of a breakthrough biosorbent for removing heavy metals from synthetic and real wastewaters in a lab-scale continuous fixed-bed column. Bioresour. Technol 229, 78–87.

Ahmad, M.F., Haydar, S., 2016. Evaluation of a newly developed biosorbent using packed bed column for possible application in the treatment of industrial effluents for removal of cadmium ions. J. Taiwan Inst. Chem. Eng. 1–10.

Amirnia, S., Ray, M.B., Margaritis, A., 2016. Copper ion removal by *Acer saccharum* leaves in a regenerable continuous-flow column. Chem. Eng. J. 287, 755–764.

Andersen, R.A., 2005. Algal Culturing Techniques. Elsevier Inc, Oxford, UK.

Beni, A.A., Esmaeili, A., 2020. Biosorption, an efficient method for removing heavy metals from industrial effluents: A review. Environ. Technol. Innov. 17, 100503.

Bulgariu, D., Bulgariu, L., 2016. Potential use of alkaline treated algae waste biomass as sustainable biosorbent for clean recovery of cadmium(II) from aqueous media: batch and column studies. J. Clean. Prod. 112 (5), 4525–4533.

Burkert, C.A.V., Barbosa, G.N.O., Mazutti, M.A., Maugeri, F., 2011. Mathematical modeling and experimental breakthrough curves of *Cephalosporin C* adsorption in a fixed-bed column. Process Biochem. 46 (6), 1270–1277.

Callery, O., Healy, M.G., 2017. Predicting the propagation of concentration and saturation fronts in fixed-bed filters. Water Res. 123, 556–568.

Chatterjee, S., Mondal, S., De, S., 2018. Design and scaling up of fixed bed adsorption columns for lead removal by treated laterite. J. Clean. Prod. 177, 760–774.

Ebisike, K., Okoronkwo, A.E., Alaneme, K.K., 2019. Adsorption of Cd (II) on chitosan–silica hybrid aerogel from aqueous solution. Environ. Technol. Innov. 14, 100337.

Escapa, C., Coimbra, R.N., Paniagua, S., García, A.I., Otero, M., 2016. Comparative assessment of diclofenac removal from water by different microalgae strains. Algal Res. 18, 127–134.

González-López, M.E., Pérez-Fonseca, A.A., Arellano, M., Gómez, C., Robledo-Ortíz, J.R., 2020. Fixed-bed adsorption of Cr(VI) onto chitosan supported on highly porous composites. Environ. Technol. Innov. 19, 100824.

Izquierdo, M., Gabaldón, C., Marzal, P., Álvarez Hornos, F.J., 2010. Modeling of copper fixed-bed biosorption from wastewater by posidonia oceanica. Bioresour. Technol 101 (2), 510–517.

Jafari, S.A., Jamali, A., 2016. Continuous cadmium removal from aqueous solutions by seaweed in a packed-bed column under consecutive sorption-desorption cycles. Korean J. Chem. Eng. 33 (4), 1296–1304.

Katırcıoğlu, H., Aslım, B., Türker, A.Rehber., Atıcı, T., Beyatlı, Y., 2008. Removal of cadmium(II) ion from aqueous system by dry biomass, immobilized live and heat-inactivated *Oscillatoria sp*. H1 isolated from freshwater (Mogan Lake). Bioresour. Technol. 99 (10), 4185–4191.

KLH, 2014. Environmental ministry's regulation of the Republic of Indonesia No. 5/2014 : waste water standard (in Indonesian).

Kumar, K.S., Dahms, H., Won, E., Lee, J., Shin, K., 2015. Microalgae – A promising tool for heavy metal remediation. Ecotoxicol. Environ. Saf. 113, 329–352.

Mazur, L.P., Pozdniakova, T.A., Mayer, D.A., Boaventura, R.A.R., Vilar, V.J.P., 2016. Design of a fixed-bed ion-exchange process for the treatment of rinse waters generated in the galvanization process using *laminaria hyperborea* as natural cation exchanger. Water Res. 90, 354–368. Muhamad, H., Doan, H., Lohi, A., 2010. Batch and continuous fixed-bed column biosorption of Cd^{2+} and Cu^{2+}. Chem. Eng. J. 158 (3), 369–377. Satya, A.,

Harimawan, A., Haryani, G.S., Johir, M.A.H., Vigneswaran, S., Ngo, H.H., Setiadi, T., 2020. Batch study of cadmium biosorption by carbon dioxide enriched aphanothece sp. dried biomass. Water 12 (1), 264.

Satya, A., Harimawan, A., Haryani, G.Sri., Setiadi, T., 2017. Non-linear isotherm models, cadmium kinetics, and biosorption thermodynamics of dried biomass of native aphanothece sp. in a batch system. J. Eng. Technol. Sci. 49 (5), 617–638.

Satya, A., Sulawesty, F., Harimawan, A., Setiadi, T., 2018. Correlation of aquatic parameters to the cadmium bioaccumulation capability onto microalgae biomass in an urban lake. J. Water Sustain. 8 (2), 59–72.

Talukdar, D., Jasrotia, T., Sharma, R., Jaglan, S., Kumar, R., Vats, R., Kumar, R., Mahnashi, M.H., Umar, A., 2020. Evaluation of novel indigenous fungal consortium for enhanced bioremediation of heavy metals from contaminated sites. Environ. Technol. Innov. 20, 101050.

Vijayaraghavan, K., Yun, Y.S., 2008. Bacterial biosorbents and biosorption. Biotechnol. Adv. 26 (3), 266–291.

Vu, H.P., Nguyen, L.N., Zdarta, J., Nga, T.T., Nghiem, L.D., 2020a. Blue-green algae in surface water: Problems and opportunities. Curr. Pollut. Rep. 6 (2), 105–122.

Vu, M.T., Vu, H.P., Nguyen, L.N., Semblante, G.U., Johir, M.A.H., Nghiem, L.D., 2020b. A hybrid anaerobic and microalgal membrane reactor for energy and microalgal biomass production from wastewater. Environ. Technol. Innov. 19, 100834.

Worch, E., 2012. Adsorption Technology in Water Treatment: Fundamentals, Processes, and Modeling. Walter de Gruyter, ISBN: 3110240238.

Xu, X., Gao, B., Tan, X., Zhang, X., Yue, Q., Wang, Y., Li, Q., 2013. Nitrate adsorption by stratified wheat straw resin in lab-scale columns. Chem. Eng. J. 226, 1–6.